Synthesis of Alkyl-Terminated Silicon Nanoclusters by a Solution Route

Chung-Sung Yang,[†] Richard A. Bley,[†] Susan M. Kauzlarich,*[,†] Howard W. H. Lee,[‡] and Gildardo R. Delgado[‡]

Contribution from the Department of Chemistry, University of California, One Shields Avenue, Davis, California 95616, and Lawrence Livermore National Laboratory, 7000 East Avenue, L-174, Livermore, California 94550

Received August 10, 1998

Abstract: We describe the synthesis and characterization of alkyl-capped nanocrystalline Si (Ĥ-*n*−Si) prepared by the reaction of $SiCl_4$ with Mg_2Si in ethylene glycol dimethyl ether (glyme) and surface-terminated with various alkyl groups, R̂-*n*−Si (R = methyl, ethyl, *n*-butyl, and *n*-octyl). This reaction produces crystalline nanoparticles with surfaces that can be chemically modified. The resultant crystalline nanoparticles can be suspended in organic solvents or isolated as a powder. The nanoclusters were characterized by transmission electron microscopy (TEM), high-resolution TEM, selected area electron diffraction (SAED), and Fourier transform infrared (FTIR) spectroscopy, electron paramagnetic resonance (EPR) spectroscopy, UV−vis absorption, and photoluminescence spectroscopy. The average cluster size depends on the reflux time of Mg_2-Si with $SiCl_4$, which provided nanoclusters with an average size of 2−5 nm. HRTEM confirms the presence of crystalline nanoclusters, and SAED is consistent with diamond-structured silicon. FTIR spectra are consistent with alkyl surface termination and show very little or no evidence for oxygen on the surface of the nanoclusters, depending on the surface alkyl group. The alkyl termination can be removed by reaction in air at 450 °C, and a Si−O stretch is observed in the FTIR spectra. EPR spectroscopy is consistent with crystalline Si nanoclusters and shows no signal at 4 K. The optical absorption spectra show an absorption edge between 260 and 240 nm, depending on the surface alkyl group, while a strong UV-blue photoluminescence between 315 and 520 nm is observed.

Introduction

Direct band gap semiconductor nanoclusters, such as group II−VI compounds, are currently the focus of intense research.[1−5] There are now well-developed synthetic routes to these nanoclusters, providing control over the size and the surface termination. In contrast, there has been little advancement in synthetic methods for the production of group IV nanoclusters, despite the large interest in nanostructured Si.[6,7] While bulk crystalline silicon luminesces very weakly, nanocrystalline forms of Si luminesce intensely over a range of wavelengths, with emission occurring primarily in the blue and the red spectral regions.[6,7] This would enable a broad range of optoelectronic applications involving efficient silicon-based emitters and has generated intense worldwide activity in this area.[6−8] Although there is a growing consensus that the luminescent centers involve Si nanoclusters, there remains controversy over the details of the light mechanism. To date, the red photoluminescence, observed in Si nanoparticles produced by a variety of methods, has been largely attributed to quantum confinement,[6,7,9,10] whereas most blue emissions have been ascribed to other sources such as oxide-related defects, molecular species, or impurities.[6]

In the past decade, a variety of fabrication techniques have been developed for silicon nanoparticles, including ultrasonic dispersion of porous silicon,[11−13] gas-phase decomposition of silanes,[10,14,15] and solution methods.[16−19] The surface of these silicon nanoparticles is passivated or terminated by hydrogen,[20] oxide,[10,14,21] or alkoxide.[17] Yields of nanoparticles are difficult

[†] University of California.
[‡] Lawrence Livermore National Laboratory.

(1) Henglein, A. *Chem. Rev.* **1989**, *89*, 1861−1873.
(2) Steigerwald, M. L.; Brus, L. B. *Annu. Rev. Mater. Sci.* **1989**, *19*, 471−495.
(3) Wang, Y.; Herron, N. *J. Phys. Chem.* **1991**, *95*, 525−532.
(4) Steigerwald, M. L.; Brus, L. E. *Acc. Chem. Res.* **1990**, *23*, 183−188.
(5) See, for example: *MRS Bull.* **1998**, *23*, 15−53.
(6) Cullis, A. G.; Canham, L. T.; Calcott, P. D. J. *J. Appl. Phys.* **1997**, *82*, 909−965.
(7) Brus, L. *J. Phys. Chem.* **1994**, *98*, 3575−3581.
(8) See, for example: *MRS Bull.* **1998**, *23*, 16−64.
(9) Vial, J. C.; Bsiesy, A.; Gaspard, F.; Hérino, R.; Ligeon, M.; Muller, F.; Romestain, R.; MacFarlane, R. *Phys. Rev. B* **1992**, *45*, 14171−14176.
(10) Brus, L. E.; Szajowski, P. F.; Wilson, W. L.; Harris, T. D.; Schuppler, S.; Citrin, P. H. *J. Am. Chem. Soc.* **1995**, *117*, 2915−2922.
(11) Heinrich, J. L.; Curtis, C. L.; Credo, G. M.; Kavanagh, K. L.; Sailor, M. J. *Science* **1992**, *255*, 66−68.
(12) Bley, R. A.; Kauzlarich, S. M.; Lee, H. W. H.; Davis, J. E. *Mater. Res. Soc. Symp. Proc.* **1994**, *351*, 275.
(13) Bley, R. A.; Kauzlarich, S. M.; Davis, J. E.; Lee, H. W. H. *Chem. Mater.* **1996**, *8*, 1881−1888.
(14) Fojtik, A.; Weller, H.; Fiechter, S.; Henglein, A. *Chem. Phys. Lett.* **1987**, *134*, 477−479.
(15) Littau, K. A.; Szajowshki, P. J.; Muller, A. J.; Kortan, A. R.; Brus, L. E. *J. Phys. Chem.* **1993**, *97*, 1224−1230.
(16) Heath, J. R. *Science* **1992**, *258*, 1131−1133.
(17) Bley, R. A.; Kauzlarich, S. M. *J. Am. Chem. Soc.* **1996**, *118*, 12461−12462.
(18) Bley, R. A.; Kauzlarich, S. M. *Synthesis of Silicon Nanoclusters*; Fendler, J. H., Ed.; Wiley-VCH: Weinheim, Germany, 1998; pp 101−118.
(19) Bley, R. A.; Kauzlarich, S. M. *A New Solution Phase Synthesis for Silicon Nanoclusters*; Fendler, J. H., Dékány, I., Eds.; Kluwer Academic Press: Dordrecht, The Netherlands, 1996; pp 467−475.
(20) Batson, P. E.; Heath, J. R. *Phys. Rev. Lett.* **1993**, *71*, 911−914.
(21) Fojtik, A.; Henglein, A. *Chem. Phys. Lett.* **1994**, *221*, 363−367.

10.1021/ja9828509 CCC: $18.00
Published on Web 05/22/1999

to determine and are typically not reported for many of these methods, with the exception of the solution techniques. The first reported solution synthesis of Si nanoclusters required high pressures and produced an estimated yield of less than 10% surface-oxidized silicon crystallites.[16] Recently, there has been a report on the solution synthesis of a high-pressure form of highly agglomerated Si nanoparticles by sonochemical methods.[22] We have reported the low-temperature solution synthesis of Si nanoclusters terminated by alkyl oxides with a similar yield.[17] This synthesis utilizes reactive Zintl salts and is performed at low temperatures without the need for high pressures. Most importantly, it provides a surface that is chemically assessable. This method of producing Si nanoclusters allows for the termination of Si nanoclusters with alkyl groups and other chemical species. The ability to chemically modify the surface of these nanoclusters provides the opportunity to study the effect of surface on the spectroscopic properties and provides an opportunity to study small Si nanoclusters with non-oxide surfaces. This paper presents the synthesis and characterization of Si nanoclusters that are terminated with alkyl groups. We have characterized these nanoclusters by high-resolution transmission electron microscopy (HRTEM), selected area electron diffraction (SAED), Fourier transform infrared (FTIR), and electron paramagnetic resonance (EPR) spectroscopies and present their absorption and photoluminescence spectra.

Experimental Section

Chemicals. Magnesium flake (99.9%) was purchased from Strem Chemical. Silicon (99.999 99+%) was obtained from J. Matthey. Semiconductor-grade $SiCl_4$ (99.99%, Aldrich) was used without further purification. Reagent-grade ethylene glycol dimethyl ether (99.5%, Aldrich) was dried by stirring with potassium overnight and distilled under argon. Grignard reagents, C_2H_5MgCl (2.0 M/diethyl ether), n-C_4H_9MgCl (2.0 M/diethyl ether), and n-$C_8H_{17}MgCl$ (2.0 M/tetrahydrofuran) were purchased from Aldrich. Methyllithium (CH_3Li, 1.6 M/diethyl ether) and n-butyllithium (n-C_4H_9Li, 1.6 M/hexane) were obtained from Acros and Aldrich, respectively. These reagents were used as supplied. HPLC grade hexane was purchased from Aldrich and used without further purification. n-tetraoctylammoniun bromide [(n-octyl)$_4$NBr, 99%+] was obtained from Aldrich and used as supplied. All reagents and materials were handled either in a nitrogen filled drybox or in a Schlenk line using standard anaerobic techniques. All glassware was silonated for 1 h with a 2% solution of dichlorodimethylsilane in toluene, then rinsed with hexane and methanol and dried at 120 °C overnight prior to use.

Synthesis. Mg_2Si was prepared by reacting Mg in a 1% excess with Si powder (99.9999%, Johnson Matthey) at 700 °C for 3 days in a sealed Nb tube, sealed in an evacuated quartz ampule, according to a literature method.[23] The product is a light blue powder and was characterized by X-ray powder diffraction. The experimental diffraction pattern agrees well with that calculated from the anti-fluorite structure for Mg_2Si.[23] No impurities were observed.

Silicon nanocrystals were produced from the reaction of 100 mg of Mg_2Si in 50 mL of ethylene glycol dimethyl ether (glyme) with excess $SiCl_4$ (0.2 mL). The mixture was refluxed for 36 or 48 h, under dry, deoxygenated argon. The blue powder does not dissolve in glyme. However, upon addition of $SiCl_4$, the blue powder gradually turns black and the solution changes from colorless to yellow-brown. (n-octyl)$_4$NBr has been investigated as a phase-transfer catalyst for increasing yields. After 36 or 48 h, the mixture is allowed to cool to room temperature and the solvent is removed under vacuum. Dried glyme is added, and subsequently methyllithium or a Grignard reagent is added via a syringe. Methyllithium (3.2 mL), n-butyllithium (2.6 mL), and the Grignard reagents C_2H_5MgCl (2.6 mL), n-C_4H_9MgCl (2.6 mL), and n-C_8H_9MgCl (2.6 mL) have been used for the termination study.

After the addition of alkyllithium or the Grignard reagent, the solution is stirred overnight to 24 h and the solvent is removed via vacuum evaporation. Water is added to dissolve and remove the salts. Hexane or cyclohexane is then added to extract the nanoparticles. The mixture is transferred to a separatory funnel and washed with water several times. The hexane colloid is clear and colorless. A pale yellow solid is observed at the hexane−water interface. Upon heating under vacuum, X-ray powder diffraction is consistent with crystalline silicon. This result suggests that this solid is amorphous silicon. The hexane is removed by air evaporation to give a sticky powder containing nanoclusters. This powder can be resuspended into hexane or cyclohexane.

The heavier powder is deep gray to black and is removed with the water. X-ray powder diffraction of this powder obtained from the water wash shows that this residue is not Mg_2Si, crystalline silicon, SiO_2, or MgOH. The major peaks in the diffraction pattern are best matched to β-$MgCl_2$. This powder does not luminesce under irradiation with UV−vis lamp.

Characterization. HRTEM samples were prepared by evaporation of colloids on lacy carbon-coated electron microscope grids. The electron microscope is a JEOL 200CX HRTEM operating with a 200 keV accelerating voltage at the National Center for Electron Microscopy (NCEM). FTIR spectra for the nanoclusters were obtained at room temperature by dropping the hexane colloid on a CsI plate and allowing the solvent to evaporate. In one experiment, the hexane colloid was placed on a NaCl plate and the solvent allowed to evaporate. After obtaining the FTIR spectrum, the sample was heated in air, on the plate, at 450 °C for 1 and 3 h, and spectra were taken. After 3 h, no further changes in the FTIR spectrum were observed. The spectra were collected on a Mattson Galaxy series FTIR 3000 spectrophotometer. EPR spectra were obtained on degassed samples of 3-methylpentane solutions of the methyl-terminated Si nanoparticles. Thee samples were transferred to a variable-temperature Dewar mounted in the EPR spectrometer (X-band and Q-band, Bruker 300E) and cooled to 4.2 K. The g-factors were calibrated by comparison to a Mn^{2+} standard in a SrO matrix ($g = 2.0012 \pm 0.0002$). The samples were checked for EPR signals, and no paramagnetic species were observed. Optical absorption spectra of the hexane or cyclohexane colloid in a quartz cell were obtained with a Hewlett-Packard 8452A diode-array spectrophotometer. Photoluminescence (PL) spectra were obtained with a Perkin-Elmer LS 50B luminescence spectrophotometer.

Results and Discussion

Metathesis reactions have been shown to be useful for synthesizing a wide variety of nanoclusters.[1−4,24−26] We have followed this approach by utilizing the high reactivity of Zintl phases such as KSi and NaGe to prepared Si and Ge nanoclusters.[17−19,27] This paper outlines our investigation of Mg_2Si as a reagent and the optimization of the reaction parameters. This phase crystallizes in the anti-fluorite structure and can be synthesize directly from the elements. It is obtained as a light blue powder. It is not as reactive as the alkali silicide phases and X-ray photoelectron spectroscopy indicates that, rather than being an ionic solid, this phase shows a great deal of covalency.[28] The reaction with $SiCl_4$ apparently produces a surface terminated with −Cl. Attempts to confirm this with FTIR spectroscopy have been inconclusive. FTIR spectra of the nanoclusters suspended in glyme show a large, broad peak between 600 and 450 cm^{-1}, and the stretch of Si−Cl is obscured. The reaction with alkyllithium or Grignard reagents produces

(22) Dhas, N. A.; Raj, C. P.; Gedanken, A. *Chem. Mater.* **1998**, *10*, 3278−3281.
(23) Li, G. H.; Gill, H. S.; Varin, R. A. *Metall. Trans. A* **1993**, *24*, 2383−2391.
(24) Kher, S. S.; Wells, R. L. *Chem. Mater.* **1994**, *6*, 2056−2062.
(25) Gillan, E. G.; Kaner, R. B. *Chem. Mater.* **1996**, *8*, 333−343.
(26) Wiley, J. B.; Kanar, R. B. *Science* **1992**, *255*, 1093−1097.
(27) Taylor, B. R.; Kauzlarich, S. M.; Lee, H. W. H.; Delgado, G. R. *Chem. Mater.* **1998**, *10*, 22−24.
(28) van Buuren, M. R. J.; Voermans, F.; van Kempen, H. *J. Phys. Chem.* **1995**, *99*, 9519−9522.

Table 1. Conditions of Surface Termination

reaction no.	weight of Mg_2Si (mg)	alkyl termination	evidence on surface	product weight (mg)
1	104.1	$-CH_3$	no O_2	8.4
2	122.3	$-C_2H_5$	no O_2	12.4
3	119.8	$-n$-C_4H_9	no O_2	14.8
4	108.4	$-n$-C_8H_{17}	little O_2	15.3
5	711.2	$-C_2H_5$	no O_2	85.4
6[a]	108.0	$-C_2H_5$	no O_2	25.2

[a] Catalyst (n-octyl)$_4$NBr has been added only in this sample.

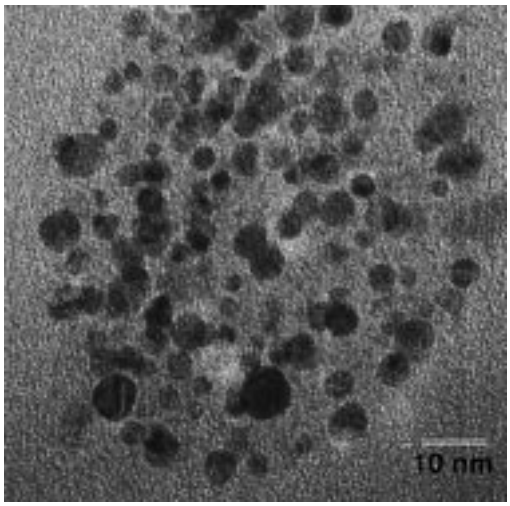

Figure 1. Typical micrograph containing a large number of silicon nanoclusters. For some of the large particles (5 nm), the outline of a hexagonal shape can be discerned.

a solid that is hydrophobic. There is no obvious difference between IR spectra of the products terminated with butyllithium and butyl Grignard reagent. This is consistent with a surface that is terminated with alkyl groups. It has been shown that this type of reaction on Si surfaces provides an alkyl surface that does not oxidize.[29−31]

The conditions of surface termination and weights of the products are provided in Table 1. The yield of nanoclusters is still low, and this is attributed to the fact that Mg_2Si is only slightly soluble in refluxing glyme. The addition of (n-octyl)$_4$NBr does not appear to change the resulting UV−vis, IR, or PL of the product. On the basis of these observations, the phase transfer catalyst aids the reaction and does not contaminate the product. The investigation of the use of diglyme, triglyme, and other solvents is in progress. It is clear that a homogeneous solution reaction will result in larger yields of crystalline Si nanoclusters.

TEM, HRTEM, and SAED were used to establish and confirm the identity of the nanoclusters isolated in hexane or cyclohexane. Figure 1 shows a micrograph for the methyl-terminated silicon nanoclusters that contain a large number of nanoclusters. The number of nanoclusters, shapes, and variety of sizes were typical for all preparations, and similar micrographs were obtained regardless of surface termination. For some of the larger particles (5 nm diameter), the outline of a hexagonal shape can be discerned. All of the reactions produced particles that showed similar images. In all cases, the SAED and lattice fringes are consistent with diamond structure Si. The sizes range

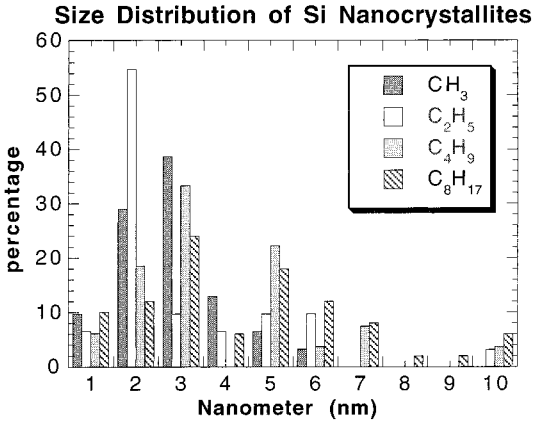

Figure 2. Size distribution of silicon nanocrystallites counted from TEM images. The average nanoparticle size ranges from 2 to 5 nm.

from 1 to 4−5 nm (diameter) for a typical synthesis with only one lattice fringe orientation dependent upon surface determination. Lattice fringes are measured from the negatives and are consistent with the {111} crystal plane of Si. Figure 2 shows the histogram of the size distributions derived from 12 TEM images that were taken from samples terminated with various alkyl groups. The average diameters of nanoparticles are 3.2 (1.3), 3.1 (1.9), 3.7 (2.1), and 4.4 (2.4) nm for $-CH_3$, $-C_2H_5$, $-n$-C_4H_9, and $-n$-C_8H_{17} termination, respectively. The standard derivation in nanoparticle size increases with the length of the alkyl chain. This suggests that the longer chain alkyl surfaces promote solubility of the larger nanoclusters.

Aggregated nanoparticles having a diameter of approximately 10−15 nm were observed in some cases, such as with n-octyl-terminated nanoclusters. The crystallites can be identified because of their different orientations of lattice fringes. The angle between lattice fringes is not consistent with a single crystal but suggests that this is an agglomeration of several small crystallites. Figure 3 shows one of the crystallites that is in the correct orientation to show lattice fringes and is outlined. The lattice fringes (3.14 Å) are consistent with the {111} crystal plane of diamond structured Si.

FTIR spectroscopy was used to identify and characterize the organic species on the cluster surfaces. In the FTIR spectra for Si clusters terminated with methyl, ethyl, n-butyl, and n-octyl alkyl groups, nine characteristic bands are observed, i.e., 2970−2960, 2920−2890, 2870−2850, 2850−2820, 1460−1450, 1380−1370, 1270−1250, 1100−1000, and 780−740 cm^{-1}. The band assignments to the functional group are taken from the literature[32−34] and provided in Table 2. The FTIR spectrum of the nanoclusters terminated with $-n$-C_8H_{17} shows a very small peak at 1100−1000 cm^{-1}, attributed to Si−O stretching.[35] This indicates either a small amount of oxygen on the surface of the nanocrystallites or the presence of a small amount of Si−O containing impurity in this sample. Nanoclusters terminated with $-CH_3$, $-C_2H_5$, and $-n$-C_4H_9 show no evidence of a Si−O stretch in the FTIR spectrum. Further evidence for the alkylation of the silicon surface is demonstrated by the oxidation of that surface at high temperatures. Figure 4 shows the FTIR spectrum for an n-butyl-terminated sample showing the characteristic

(29) Linford, M. R.; Fenter, P.; Eisenberger, P. M.; Chidsey, C. E. D. *J. Am. Chem. Soc.* **1995**, *117*, 3145−3155.
(30) Bansal, A.; Li, X.; Lauermann, I.; Lewis, N. S. *J. Am. Chem. Soc.* **1996**, *118*, 7225−7226.
(31) Terry, J.; Linford, M. R.; Wigren, C.; Cao, R.; Pianetta, P.; Chidsey, C. E. D. *Appl. Phys. Lett.* **1997**, *71*, 1056−1058.
(32) Lin, W. L.; Tsai, H. K.; Lee, S. C.; Sah, W. J.; Tzeng, W. J. *Appl. Phy. Lett.* **1987**, *51*, 2112−2114.
(33) Socrates, G. *Infrared Characteristic Group Frequencies*; Wiley: New York and London, 1980.
(34) Chen, J. H.; Sah, W. J.; Lee, S. C. *J. Appl. Phys.* **1991**, *70*, 125−130.
(35) Green, W. H.; Le, K. P.; Grey, J.; Au, T. T.; Sailor, M. J. *Science* **1997**, *276*, 1826−1828.

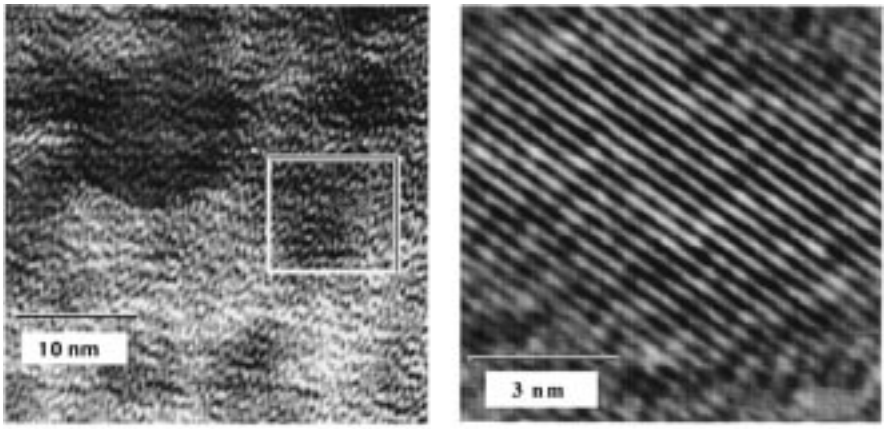

Figure 3. (a) HRTEM image showing the silicon nanoclusters terminated with methyl groups. (b) Rotationally filtered image of $(Si)_x-CH_3$. *D*-spacings of these lattice fringes are consistent with the {111} silicon crystal plane (3.14 Å).

Table 2. Characteristic Peak Groups Observed in $(Si)_x-R$ IR Spectra [R = $-CH_3$, $-C_2H_5$, $-n$-C_4H_9, $-n$-C_8H_{17} (s = strong, m = medium, w = weak)]

wavenumbers	functional group assigned
2970−2960 (m)	C−CH_3 or Si−CH_3 terminal $-CH_3$ group asymmetricalstretching
2920−2890 (s)	C−CH_2 asymmetric stretching
2870−2850 (w)	C−CH_3 or Si−CH_3 terminal $-CH_3$ group symmetric stretching
2850−2820 (s)	C−CH_2 symmetric stretching
1460−1450 (m)	C−CH_3 or Si−CH_3 deformation or Si−CH_2 scissor
1360−1340 (w)	C−H deformation or bending
1270−1250 (w)	Si−CH_3 or Si−CH_2 symmetric bending
1100−1000 (m)	Si−OR stretching
780−740 (w)	Si−CH_3 rocking or wagging

frequencies for C−H modes. This sample was then heated in air at 450 °C for 1 and 3 h. All of the modes attributed to C−H decrease as the Si−O stretching mode found between 1100 and 1000 cm^{-1} increases. The FTIR spectra clearly show the removal of the alkyl groups and the development of an oxide-terminated surface and subsequent oxidation to SiO_2. EPR spectroscopy results on the methyl-terminated sample further support the absence of paramagnetic species on the nanocluster surface. Therefore, the defect-related paramagnetic centers, such as damaged crystalline, amorphous Si, or dangling bonds, are not expected to be found in our samples.[36] This indicates well-controlled surfaces and complete passivation with alkyl groups.

Optical absorption and PL spectroscopy were used to investigate the optical properties of these silicon nanoclusters. The UV−vis absorption spectra of various colloids are shown in Figure 5. The absorption of the solvent (hexane) has been subtracted from each of the spectra. The nanocluster colloids show similar features in the optical spectra. These spectra are similar to Si nanoparticles of similar diameter with an oxide surface.[15] There is an absorption at approximately 280 nm in the spectrum of the four samples. This is not observed in silicon nanoparticles with an oxide surface, where a continuous absorption in the blue is observed.[15] The optical intensity of this absorption is proportional to the concentration of the hexane colloid. Size-selected precipitation of nanoclusters and further studies of the optical properties will provide insight into the identification of this feature. An absorption edge appears at approximately 390 nm for the *n*-butyl, and *n*-octyl-terminated samples and at 360 nm for the methyl- and ethyl-terminated nanoclusters, which is considerably blue-shifted from the band gap of bulk Si. The absorption edge shifts with nanocluster size in accordance with quantum confinement models and agrees with sizes observed in TEM images.

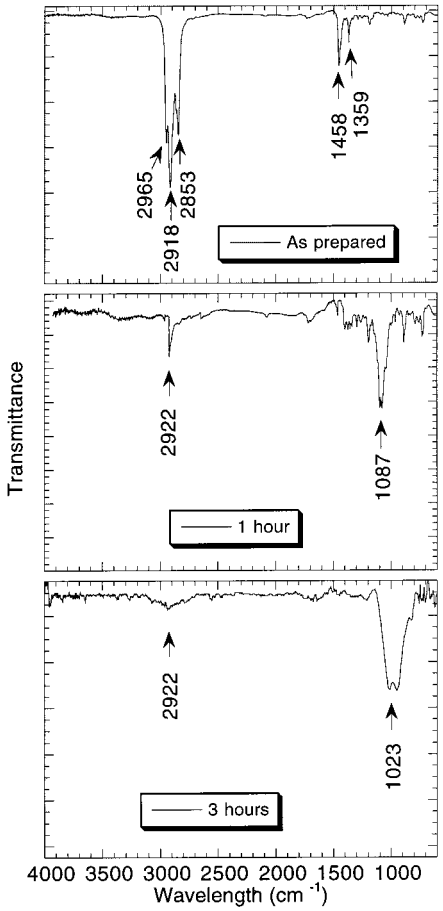

Figure 4. FTIR spectra for silicon nanoclusters terminated with *n*-butyl groups as prepared and oxidized in air 450 °C for 1 and 3 h.

The photoluminescence spectra were measured at room temperature. The emission spectra were collected with an excitation wavelength of 310 nm and a spectral resolution of 2.5 nm, as shown in Figure 6. All emission spectra contained a peak centered between 360 and 390 nm (3.4−3.2 eV) that

(36) Uchida, Y.; Koshida, N.; Koyama, H.; Yamamoto, Y. *Appl. Phys. Lett.* **1993**, *63*, 961−963.

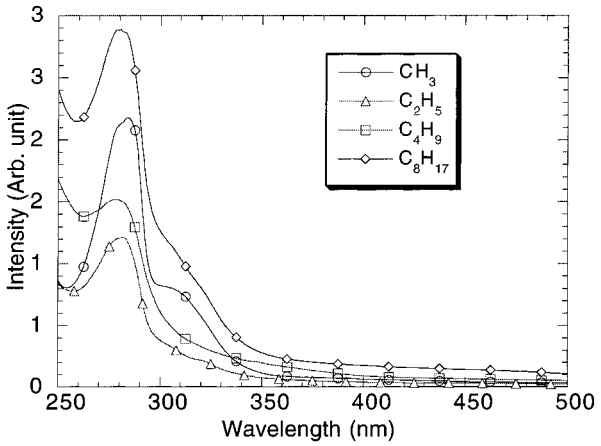

Figure 5. UV−vis spectra for silicon nanoclusters terminated with alkyl groups. Absorbance begins at 390 nm and increases toward lower wavelengths for the *n*-butyl- and *n*-octyl-terminated samples and at 360 nm for the methyl- and ethyl-terminated nanoclusters.

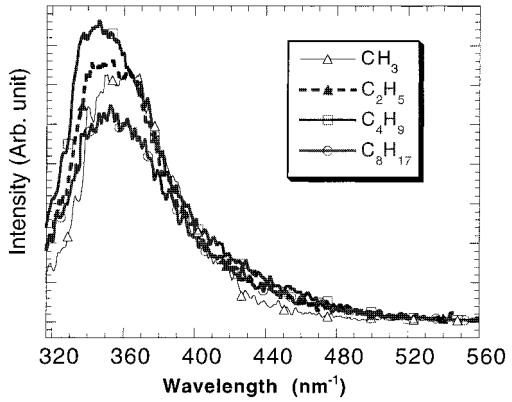

Figure 6. PL spectra for alkyl-terminated silicon nanoclusters. These emission spectra were collected from 300 to 800 nm with an excitation bandwidth of 2.5 nm and excitation wavelength of 310 nm.

corresponds to greater than the bulk band gap energy. This UV-blue PL from these nanocrystallites occur in a different spectral region than that from other blue emitters such as oxidized porous silicon (440−480 nm)[37,38] or silicon carbide (500−520 nm),[39] thus complimenting their blue output performance. The intensity of the blue PL from these nanoparticles is affected by the cluster size and depends linearly on the excitation power density.[40,41] It is expected that luminescence from traps in semiconductors will saturate at high excitation powers due mainly to their lower number density relative to the band edge states of semiconductor. As a result, the observation of a linear dependence of the luminescence intensity as a function of excitation power indicates that saturation does not occur. This suggests that the origin of the luminescence is less likely to be from traps, such as oxide or defect sites. The intensity dependence of the photoluminescence is more consistent with quantum confinement, rather than defects.

To date, the origin of blue PL from nanocrystalline Si systems remains controversial.[6] A variety of explanations have been suggested, including quantum confinement, impurities, oxide-related species, surface states, molecular species, and amorphous Si. More detailed spectroscopy, including time-resolved studies, will be the subject of another publication.[41] This work suggests that the blue PL in these nanoclusters is not due to defects.

Summary

We report on a convenient and versatile technique for the synthesis of a variety of R̂-*n*−Si compounds and have systematically characterized them. FTIR spectra are consistent with a nanocluster surface that is alkyl-terminated. Reaction of Bu-*n*-Si at 450 °C with air results in removal of the alkyl groups and oxidation to SiO_2. There is no evidence of oxygen in the case of the methyl-, ethyl-, and *n*-butyl-terminated nanoclusters. This implies well-controlled surfaces and complete passivation with alkyl groups. However, in *n*-octyl-terminated nanoclusters, a small amount of oxygen may be present on the surface or as an impurity in the sample. HRTEM shows that the nanocrystallite sizes are primarily in the range of 2−5 nm and that crystallites with long alkyl chains may agglomerate in solution. PL spectra of the nanoclusters show a strong UV-blue PL between 315 and 520 nm, and its intensity depends linearly on the excitation power density. The UV-blue PL could be observed in silicon nanoclusters with or without oxygen on the surface, indicating that surface oxide constituents are not responsible for the UV-blue PL. These results suggest that the observed UV-blue emission is consistent with optical transitions in quantum-confined silicon nanoclusters.

Acknowledgment. We thank Tijana Rajh (ANL) for the EPR study. We acknowledge useful discussion with Tijana Rajh and Ric Kaner (UCLA). We thank the staff at the National Center for Electron Microscopy (NCEM) for useful discussion and assistance with the HRTEM. Work at the NCEM was performed under the auspices of the Director, Office of Energy Research, Office of Basic Energy Science, Materials Science Division, U.S. Department of Energy, under Contract DE-AC-03-76XF00098. This work has been supported by the National Science Foundation (Grant DMR-9505565, DMR-9803074) and the Campus Laboratory Collaboration Program of the University of California. Work at the Lawrence Livermore National Laboratory was performed under the auspices of the U.S. DOE under Contract No.W-7405-ENG-48 and was supported by the Laboratory Directed Research and Development Program at LLNL.

JA9828509

(37) Canham, L. T.; Loni, A.; Calcott, P. D. J.; Simons, A. J.; Reeves, C.; Houlton, M. R.; Newey, J. P. *Thin Solid Films* **1996**, *276*, 112−115.
(38) Koyama, H.; Matsushita, Y.; Koshita, N. *J. Appl. Phys.* **1998**, *83*, 1776−78.
(39) Konstantinov, A. O.; Henry, A.; Harris, C. I.; Janzen, E. *Appl. Phys. Lett.* **1995**, *66*, 2250−2252.
(40) Zhao, X.; Schoenfield, O.; Kumuro, S.; Aoyagi, Y.; Sugano, T. *Phys. Rev. B.* **1994**, *50*, 18654−18657.
(41) Lee, H. W. H.; Degado, G. R.; Taylor, B. R.; Mayeri, D.; Yang, C.-S.; Kauzlarich, S. M. Manuscript in preparation.